

1-1-2023

Voltammetric determination of inorganic arsenic in mildly acidified (pH 4.7) groundwaters from Mexico and India

Martijn Eikelboom

Yaxuan Wang

Gemma Portlock

Arthur Gourain

Joseph Gardner

See next page for additional authors

Follow this and additional works at: <https://ro.ecu.edu.au/ecuworks2022-2026>



Part of the [Water Resource Management Commons](#)

[10.1016/j.aca.2023.341589](https://doi.org/10.1016/j.aca.2023.341589)

Eikelboom, M., Wang, Y., Portlock, G., Gourain, A., Gardner, J., Bullen, J., . . . Salaun, P. (2023). Voltammetric determination of inorganic arsenic in mildly acidified (pH 4.7) groundwaters from Mexico and India. *Analytica Chimica Acta*, 1276, article 341589. <https://doi.org/10.1016/j.aca.2023.341589>

This Journal Article is posted at Research Online.

<https://ro.ecu.edu.au/ecuworks2022-2026/2887>

Authors

Martijn Eikelboom, Yaxuan Wang, Gemma Portlock, Arthur Gourain, Joseph Gardner, Jay Bullen, Paul Lewtas, Matthieu Carriere, Alexandra Alvarez, Arun Kumar, Shane O'Prey, Tamás Tölgyes, Dario Omanović, Subhamoy Bhowmick, Dominik Salaun, and Pascal Salaun



Voltammetric determination of inorganic arsenic in mildly acidified (pH 4.7) groundwaters from Mexico and India

Martijn Eikelboom^{a,*}, Yaxuan Wang^a, Gemma Portlock^a, Arthur Gourain^a, Joseph Gardner^a, Jay Bullen^b, Paul Lewtas^c, Matthieu Carriere^d, Alexandra Alvarez^d, Arun Kumar^e, Shane O'Prey^f, Tamás Tölgyes^f, Dario Omanović^g, Subhamoy Bhowmick^h, Dominik Weiss^b, Pascal Salaun^{a,**}

^a School of Environmental Sciences, University of Liverpool, 4 Brownlow Street, L69 3GP, Liverpool, UK

^b Department of Earth Science and Engineering, Imperial College London, South Kensington Campus, London, SW7 2AZ, UK

^c School of Science, Edith Cowan University, 270 Joondalup Drive, Joondalup, Western Australia, 6027, Australia

^d Caminos de Agua, José María Correa 23A, Colonia Santa Cecilia, 37727, San Miguel de Allende, Gto, Mexico

^e Mahavir Cancer Sansthan and Research Centre, Phulwarisharif, Patna, 801505, Bihar, India

^f Informatic Component Technology, UK

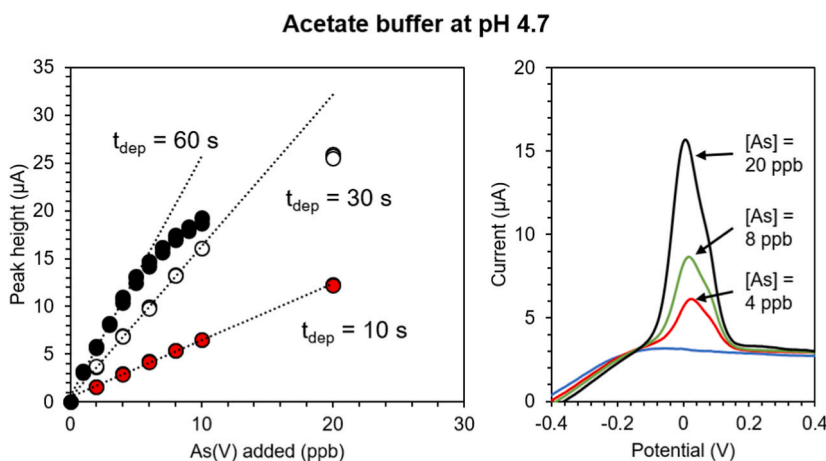
^g Division for Marine and Environmental Research, Ruder Bošković Institute, Bijenička 54, 10000, Zagreb, Croatia

^h Kolkata Zonal Center CSIR-National Environmental Engineering Research Institute (NEERI), Kolkata, West Bengal, 700107, India

HIGHLIGHTS

- Novel methodology for detection of inorganic arsenic at various pH.
- Arsenic analysis in reduced groundwaters of West Bengal and oxidised groundwater of Central Mexico.
- Comparison study between voltammetric determination in acidic conditions vs. near-neutral pH.
- Validation study between voltammetric methods with inductively coupled plasma mass spectrometry (ICP-MS).
- Scanning electron microscope image of gold microwire surface.

GRAPHICAL ABSTRACT



ARTICLE INFO

Handling Editor: Prof Lin Yuehe

ABSTRACT

Routine monitoring of inorganic arsenic in groundwater using sensitive, reliable, easy-to-use and affordable analytical methods is integral to identifying sources, and delivering appropriate remediation solutions, to the

* Corresponding author.

** Corresponding author.

E-mail addresses: martijn.eikelboom@liverpool.ac.uk (M. Eikelboom), salaun@liv.ac.uk (P. Salaun).

<https://doi.org/10.1016/j.aca.2023.341589>

Received 30 March 2023; Received in revised form 19 June 2023; Accepted 4 July 2023

Available online 4 July 2023

0003-2670/© 2023 The Authors. Published by Elsevier B.V. This is an open access article under the CC BY license (<http://creativecommons.org/licenses/by/4.0/>).

Keywords:

Inorganic arsenic
Arsenate
Groundwater
Anodic stripping voltammetry
Gold microwire electrode

widespread global issue of arsenic pollution. Voltammetry has many advantages over other analytical techniques, but the low electroactivity of arsenic(V) requires the use of either reducing agents or relatively strong acidic conditions, which both complicate the analytical procedures, and require more complex material handling by skilled operators. Here, we present the voltammetric determination of total inorganic arsenic in conditions of near-neutral pH using a new commercially available 25 μm diameter gold microwire (called the Gold Wirebond), which is described here for the first time. The method is based on the addition of low concentrations of permanganate (10 μM MnO_4^-) which fulfils two roles: (1) to ensure that all inorganic arsenic is present as arsenate by chemically oxidising arsenite to arsenate and, (2) to provide a source of manganese allowing the sensitive detection of arsenate by anodic stripping voltammetry at a gold electrode. Tests were carried out in synthetic solutions of various pH (ranging from 4.7 to 9) in presence/absence of chloride. The best response was obtained in 0.25 M chloride-containing acetate buffer resulting in analytical parameters (limit of detection of 0.28 $\mu\text{g L}^{-1}$ for 10 s deposition time, linear range up to 20 $\mu\text{g L}^{-1}$ and a sensitivity of 63.5 nA $\text{ppb}^{-1} \cdot \text{s}^{-1}$) better than those obtained in acidic conditions. We used this new method to measure arsenic concentrations in contrasting groundwaters: the reducing, arsenite-rich groundwaters of India (West Bengal and Bihar regions) and the oxidising, arsenate-rich groundwaters of Mexico (Guanajuato region). Very good agreement was obtained in all groundwaters with arsenic concentrations measured by inductively coupled plasma-mass spectrometry (slope = +1.029, $R^2 = 0.99$). The voltammetric method is sensitive, faster than other voltammetric techniques for detection of arsenic (typically 10 min per sample including triplicate measurements and 2 standard additions), easier to implement than previous methods (no acidic conditions, no chemical reduction required, reproducible sensor, can be used by non-voltammetric experts) and could enable cheaper groundwater surveying campaigns with in-the-field analysis for quick data reporting, even in remote communities.

1. Introduction

Arsenic pollution of groundwater is a global issue and the extent of the problem is reflected in the large number of scientific articles published over the past decades. Health effects linked to consumption of food and water containing elevated arsenic exposure include increased risk of cancer, skin lesions, mental disabilities and diabetes [1–3]. The Bengal Delta Plain, in Bangladesh and West Bengal, experiences particularly severe arsenic contamination of groundwater aquifers, with concentrations as high as 4600 $\mu\text{g L}^{-1}$ (ppb), 460 times higher than the 10 $\mu\text{g L}^{-1}$ World Health Organization (WHO) guideline [4,5]. Roughly 70–80 million and 28–60 million people are exposed to elevated arsenic concentrations in India and Bangladesh, respectively [6]. Other countries in South East Asia experiencing severe arsenic contamination include Cambodia, China, Myanmar, Nepal, Pakistan and Vietnam. In the Americas, impacted countries include Mexico, with 6–9 million people exposed to elevated levels of arsenic through drinking water [2, 7]. The national standard for arsenic in drinking water is 50 $\mu\text{g L}^{-1}$ in Bangladesh [7], while Mexico and India recently adopted the WHO guideline of 10 $\mu\text{g L}^{-1}$ [8]. However, the health effects of chronic exposure to arsenic concentrations below 10 $\mu\text{g L}^{-1}$ are still uncertain [9], motivating Dutch drinking water companies to aim to decrease the concentration of arsenic to below 1 $\mu\text{g L}^{-1}$ [10]. Arsenic exposure arises from food as well as water, and recent studies have shown significant arsenic exposure due to rice irrigated or washed with arsenic contaminated groundwater [11].

It is generally accepted that reductive dissolution from iron oxyhydroxides is the main mechanism behind the high arsenic concentration in West Bengal and Bangladesh groundwater [12,13]. In contrast, hypotheses for the mechanism of arsenic release into central Mexico's aquifers include the oxidative dissolution of arsenic bearing pyrite and scorodite, and geothermally induced hydrolysis of silicate [14,15]. These reductive and oxidative arsenic release mechanisms consequently lead to South Asian groundwaters mainly containing arsenite As(III) with high concentrations of dissolved iron and manganese (up to 8.0 mg L^{-1} and 2.4 mg L^{-1} respectively) and Mexican groundwaters mainly containing As(V) (with low concentrations of iron and manganese) [16].

The importance of arsenic monitoring in groundwater wells is well-recognised, as arsenic concentrations are known to fluctuate spatially and temporally [17]. The arsenic species found in groundwater are predominantly inorganic, i.e. the reduced arsenite, H_3AsO_3 , and oxidised arsenate, H_3AsO_4 . The organic forms monomethylarsonic acid [MMA; $\text{CH}_3\text{AsO}_3\text{H}_2$], and dimethylarsenate acid [DMA; $(\text{CH}_3)_2\text{AsO}_2\text{H}$],

are usually present only in small abundances [18]. Inorganic arsenic is considered to be more toxic than the organic arsenic species, and inorganic As(III) is more toxic than inorganic As(V) [19].

Quantification of total As [the sum of As(III) and As(V)] and arsenic speciation (i.e. the ratio between As(III) and As(V)) can be performed through various analytical techniques. Inductively coupled plasma mass spectrometry (ICP-MS) is a sensitive arsenic detection technique with low detection limits and may be used in combination with liquid separation techniques such as high pressure liquid chromatography (HPLC) to distinguish between different arsenic species [20]. Atomic absorption spectroscopy (AAS) and atomic emission spectroscopy (AES) offer highly sensitive detection of arsenic species, and are cheaper compared to ICP-MS instrumentation and running costs [21]. However, both methods rely on equipment too bulky to facilitate on-site and/or remote detection of arsenic, are complex in terms of maintenance, and instrumentation costs are £20,000–100,000 [22]. Electrochemical detection of arsenic, e.g. with anodic stripping voltammetry (ASV) can provide a viable alternative technique as it is sensitive and selective towards a range of trace metals [16,23–35]. The ASV analytical procedure is simple to operate, requires low cost instrumentation (e.g. 2–10 times cheaper than AAS, and 20–100 times cheaper than ICP-MS) with low power consumption, maintenance issues can be easily fixed by the operator (e.g. replacing electrodes) in comparison to ICP-MS, and lightweight instruments which are well suited for on-site determination of arsenic [36].

During a typical ASV procedure, inorganic arsenic is first reduced and accumulated onto an electrode surface as solid phase As(0) during the deposition step. As(0) is then oxidised to As(III) during the stripping step, creating an increase in current at the peak potential which is directly proportional to the initial aqueous phase arsenic concentration of the sample (when measurements are made within a certain linear range) [28]. The range of electrode materials compatible with ASV detection of arsenic includes gold [24], carbon [37], diamond [38], silver [39], as well as electrode modifications (e.g. gold nanoparticles [40], organic molecules [41]), electrode type (wire [25], disc [42], screen-printed [43]), and electrolytes (hydrochloric acid at pH 2 [44], HEPES in seawater at pH 7–8 [25], phosphate in synthetic water at pH 7.4 [45], sulphite in alkaline conditions [33]). However, total arsenic detection by voltammetry using gold electrodes is typically performed under acidic conditions using very negative deposition potentials to facilitate the reduction of the hydrolysed species (H_3AsO_4 and H_2AsO_4^-) [28]. Limitations related to acidic conditions include safety considerations (especially during transportation to field sites), electrode

lifetimes limited by corrosion, and potential interference from hydrogen [46]. Detection of total arsenic at neutral pH was long thought to be impossible due to As(V) being considered as electro-inactive [47], i.e. impossible to reduce electrochemically. Consequently, early methods included a pre-analysis step, reducing As(V) to As(III) with chemical reducing agents (e.g. sodium sulphite [48], sulphur dioxide [49] or L-cysteine [50]). Reductive pre-treatments complicate the analytical procedure and limit sample throughput as they require 5–60 min reaction time, heating, and deaeration. However, As(V) is electroactive in acidic conditions [28], which avoids the use of reducing agents but requires the addition of acid. The direct detection of As(V) in non-acidic conditions has only been achieved on rare occasions [25,32,35,51]. It was first achieved in seawater, at pH 8 [25]. The method described was based on the chemical reduction of As(V) facilitated by Mn(0) at the gold surface during the deposition step and requires the addition of Mn(II) and hypochlorite (to oxidise all As(III) to As(V)) in buffered deoxygenated seawater. The sensitivity (i.e. the current generated by a given concentration of arsenic at a given deposition time) and detection limits are similar to those obtained in acidic conditions. These near-neutral pH methods are advantageous by offering new insights into arsenic mobility in the environment; this was demonstrated in estuarine conditions where the inorganic As levels detected at neutral pH were significantly lower than in acidic conditions [51]. These results were used to suggest that some As(V) present in the dissolved fraction was adsorbed onto colloidal species, likely reducing bioavailability [51].

In this work, we present a new methodology for the detection of total inorganic arsenic in groundwater in non-acidic conditions. It is based on ASV at a gold microwire electrode in the presence of permanganate (MnO_4^-), which may be advantageous over the method using Mn(II) [25] as it fulfils two roles: (1) oxidising As(III) to As(V) to ensure that the total arsenic detection method has equal sensitivity to both arsenic species; and (2) it is reduced to Mn(0) at the gold surface during the deposition step, allowing the subsequent chemical reduction of As(V) to As(0) at this pH. The method was developed and optimised using a new manufactured gold wire electrode sensor which is presented here for the first time. There are several advantages in regards to using a wire electrode over disk or screen-printed electrodes. Firstly, a higher diffusion flux is achieved as the diffusion layer of a cylindrical 25 μm wire is approximately 2 μm [27], leading to lower detection limits. Secondly, no mechanical polishing is required. Instead, a fast and easy electrochemical cleaning procedure in sulfuric acid is used which cannot be used at a disk electrode due to the formation of hydrogen bubbles. Thirdly, it allows analysis of solutions in conditions of pH and deposition potential that are not accessible to the disk electrodes [26]. We present here the development of the method (optimum MnO_4^- concentration, effect of various halogens and buffers, interferences from Cu, Fe or humic substances) and analytical parameters (i.e. linear range, sensitivity, detection limit) obtained at varying pH (from 1 to 9). Finally, we tested the method by measuring arsenic concentration in groundwater samples from Mexico and India and compared our voltammetric results at pH 4.7 with (a) results obtained in acidic conditions (pH 1) and (b) results obtained by ICP-MS as benchmark methods. We finally discuss the advantages and limitations of this methodology, both in analytical performance and in user friendliness/conviviality.

2. Experimental

2.1. Reagents

The water used to prepare reagents and working solutions was purified to $18 \text{ M}\Omega \text{ cm}^{-1}$ using a Millipore-Elix system. During fieldwork in Mexico, demineralized water was used ($>1 \text{ M}\Omega \text{ cm}^{-1}$). In India, distilled water from Merck was used with a resistivity of $18 \text{ M}\Omega \text{ cm}^{-1}$. A total arsenic standard (1000 mg L^{-1}) was prepared by dissolving the appropriate amount of disodium arsenate heptahydrate ($\text{Na}_2\text{HAsO}_4 \cdot 7\text{H}_2\text{O}$, CAS: 10048-95-0, Sigma-Aldrich) in water (H_2O) and acidified to pH 2

using 1 M HCl. A 1 M HCl solution was prepared from concentrated hydrochloric acid (38%, CAS: 7647-01-0, Sigma-Aldrich) in Liverpool, (36.5–38%, CAS: 7647-01-0, Karal) in Mexico, and (35–37%, Qualigem, CAS: 7647-01-0) in India.

An acetate buffer (referred to as CLAC electrolyte, pH 4.7) was prepared by dissolving 7.3 g sodium chloride ($>99\%$, CAS: 7647-14-5, Sigma-Aldrich), 2.34 g sodium acetate trihydrate (CAS: 6131-90-4, Karal), and 0.6 mL acetic acid ($>99\%$, CAS: 64-19-7, Sigma-Aldrich) in 500 mL demineralized water. The final concentrations in the electrochemical cell were: 0.25 M NaCl and 80 mM acetate. 10 mM acetate, phosphate, borate, HEPES and TES buffers were prepared by dissolving $\text{C}_2\text{H}_3\text{NaO}_2$ (BDH), Na_2HPO_4 (BDH), $\text{Na}_2[\text{B}_4\text{O}_5(\text{OH})_4] \cdot 8\text{H}_2\text{O}$ (Sigma-Aldrich), $\text{C}_8\text{H}_{18}\text{N}_2\text{O}_4\text{S}$ (HEPES, Acros, 99%, CAS: 7365-45-9), $\text{C}_6\text{H}_{15}\text{NO}_6\text{S}$ (TES, Fisher, 98%, CAS: 7365-44-8) in water, respectively.

A solution of 0.5 M sulfuric acid (H_2SO_4) was prepared from concentrated sulfuric acid (98%, CAS: 7664-93-9) from Sigma-Aldrich in Liverpool, from Karal in Mexico, and from Merck in India. A 10 mM potassium permanganate standard was prepared by dissolving KMnO_4 into demineralized water ($>99\%$, CAS: 7722-64-7, Karal) in Mexico, and (98.5%, Merck, CAS: 7722-64-7) in India. A solution of 3 M potassium chloride (CAS: 7447-40-7, Sigma-Aldrich), and a solution 5 g/L ethylenediaminetetraacetic acid anhydrous ($\text{C}_{10}\text{H}_{16}\text{N}_2\text{O}_8$, EDTA, CAS: 60-00-4, Sigma-Aldrich) were prepared in demineralized water. 1 M NaCl (BDH), 1 M NaBr (Fisher), 1 M KI (BDH) were used for the halogen experiments. Analytical standards were used for studying Cu (1000 mg L^{-1} , Fluka), Fe (1000 mg L^{-1} , BDH), Mn (1000 mg L^{-1} , BDH). 5 M nitric acid was prepared to acidify samples for ICP-MS analysis (69–71%, Thermo Fisher, CAS: 7784-46-5). All solutions were kept at room temperature, except for the As(III) standard, which was kept in the dark at $+3^\circ\text{C}$.

For analysing humic substances, molybdenum Mo(VI) standard solutions ($10 \mu\text{M}$) were prepared by diluting atomic absorption spectroscopy standard solutions of 1 g/L (Fisher Scientific) in 10 mM HCl. Fulvic acid (FA) from the Suwannee River (International Humic Substances Society, IHSS standard) was dissolved in Milli-Q to a concentration of 10 mg L^{-1} . Deep Sea Reference (DSR) seawater (Batch 20–2020 – Lot 08–20 and Batch 21–2021 – Lot 08–18) with certified dissolved organic carbon (DOC) concentrations of 44–46 μM were obtained from Hansell laboratory in Miami. SRFA standard and DSR samples were always kept in the dark and refrigerated when not in use.

2.2. Electrode fabrication, description and conditioning

The Gold WireBond sensor (gold wire working electrode) (Fig. 1) were manufactured by Informatic Component Technology, UK, using the technique of wire bonding. A 1 mm thick sheet of alumina was first machined to create connecting pads, 0.25 mm groove channels and small cavities (5 by 2 mm) before being cleaned by an acid/alkaline/MilliQ bath followed by an oxygen plasma cleaning. Gold was deposited by sputtering, covering the entire area of the alumina. Top layers were removed, leaving the gold only in the channels and pads. Individual electrodes were cut out from the alumina sheet and for each electrode, a gold wire (Goodfellows, hard, 99% purity) was wire-bonded to the sputtered gold within the groove channels from one side of the cavity to the other. Finally, each electrode was manually encapsulated with a chemically-resistant epoxy that covered the entire electrode but the pads and gold wire. Each gold wire is 5 mm long and has a diameter of 25 or 30 μm . The electroactive surface area, measured by cyclic voltammetry [52], was found to be reproducible (less than 2% relative standard deviation, $N = 6$). The cavity was designed to ensure optimum hydrodynamics around the wire when the solution is stirred and the Gold Wirebond was placed perpendicular to the flow. The entire sensor is c. a. 65 mm long and 5 mm wide, fitting inside a standard voltammetric cell. The contact with the potentiostat is made with a crocodile clip connected onto the gold pad.

The electrode was conditioned daily, consisting of rapid

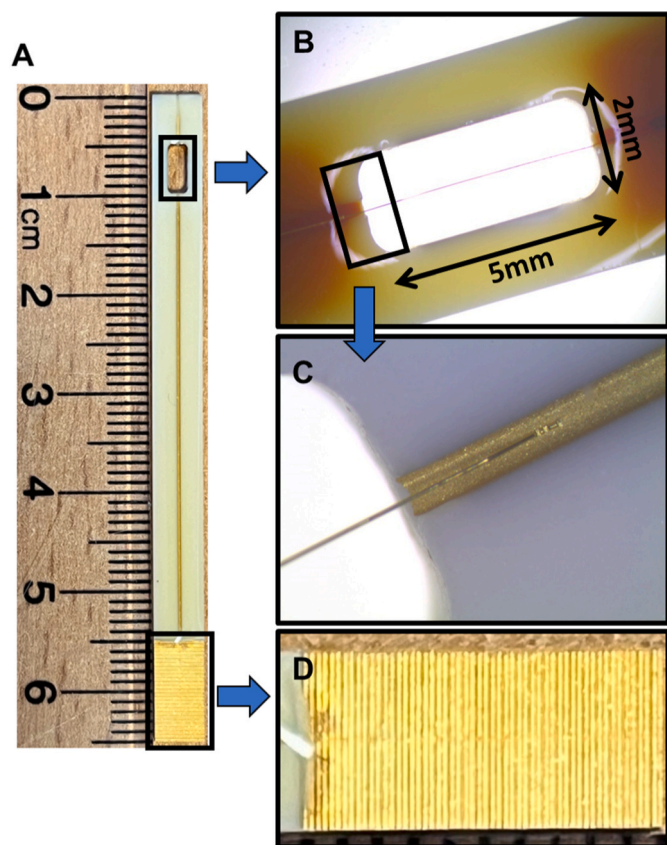


Fig. 1. A: The gold microwire electrode. B: Electroactive surface area of the gold wire (length 5 mm) and opening with encapsulation with chemically resistant resin; C: Wire-bonded gold on the gold track; D: The gold pad which makes the connection to the potentiostat with a crocodile clip. (For interpretation of the references to colour in this figure legend, the reader is referred to the Web version of this article.)

electrochemical cleaning (holding the working electrode potential at -2 V for 10 s) in 0.5 M H_2SO_4 , similar to previously reported [52]. This cleaning step helps maintain a clean and reproducible electroactive gold surface and can be seen as a reset of the electrode, in the same way as polishing is used for disc electrodes.

2.3. Groundwater sampling

Mexican groundwater samples were collected during September and October 2021 in the state of Guanajuato, from wells ($N = 8$) and water re-fill locations ($N = 3$) in multiple rural communities and areas surrounding the city of San Miguel de Allende, at the following locations (Table S1): Atotonilco, San Luis Rey, Puerto de Nieto, Sosnabar, La Esparanza, San Antonio de Lourdes, Pozo Hondo, and Ex Hacienda de Jesus. Groundwater was pumped for 5 min to purge the well of stale water and samples for voltammetry analysis were collected in 0.5 L Nalgene bottles, filtered with a 0.45 μm membrane filter (Millex-HV Syringe Filter Unit, PVDF, 33 mm, gamma sterilized), and stored in the fridge at $+3$ °C within a few hours of sampling. Total dissolved solids (TDS) and conductivity were measured on-site with a Health Metric TDS&EC meter, and the pH was determined with a Hach Pocket Pro pH Tester, which was previously calibrated using buffer solutions at pH 4.01, 6.86 and 9.18. Groundwater samples for inductively coupled plasma mass spectrometry (ICP-MS) analysis were collected in 15 mL acid washed sample tubes (Centrifuge tubes, CN series) and immediately acidified to pH 2 with 0.01 M nitric acid. These samples were collected unfiltered and filtered, with 0.45 , 0.2 , or 0.02 μm (Whatman, Anotop 25) syringe filters (0.2 and 0.02 μm filtrate was obtained from the 0.45

μm filtrate).

Indian groundwater samples were taken in 2019 ($N = 30$) and 2022 ($N = 15$) from individual and community hand wells, in Chakdaha block, West Bengal and in the village of Chapar, Bihar. Groundwater was pumped for a minimum of 5 min before samples were collected. Filtering was performed immediately after sampling to avoid any precipitation of iron oxides. Filtration at 0.45 , 0.2 and 0.02 μm was performed using the Millex-HV Syringe Filter Unit and Anotop filters. In contrast to the sampling in Mexico, HCl (0.01 M) or EDTA (1 mM in 2022 and 10 mM in 2019) was added to the samples, immediately after filtration, to prevent any precipitation (e.g. of iron oxides) [16]. Filtered groundwater samples intended for ICP-MS analysis were collected in 15 mL acid-washed sample tubes (centrifuge tubes, CN series) and immediately acidified to pH 2 with 0.1 M nitric acid. Temperature, conductivity and pH were determined on site with a Hanna Instruments HI 98129 pH Meter. GPS coordinates were recorded at every groundwater well. The depth of wells was recorded when provided by locals. Table S1 lists all sampling stations in Mexico and India.

2.4. Arsenic determination by voltammetry

Electrochemical measurements were performed in 30 mL plastic cups using a portable PDV6000 Ultra Potentiostat (Modern Water, UK) controlled with VAS software (version 4.7). The electrochemical cell was equipped with a silver/silver chloride reference electrode placed in a double bridge filled with 3 M KCl, an auxiliary platinum electrode, and the Gold WireBond working electrode. Between the three electrodes was a stirrer which was operated through the software. The whole electrochemical setup was portable and designed for on-site analysis (see Fig. S1 in the supplementary document). The gold wire electrode used in Mexico was 25 μm in diameter and both 25 and 30 μm diameter electrodes were used in India. Arsenic concentrations were measured by the method of standard additions [53], with a minimum of 3 measurements for the sample (until the signal was stable) and typically triplicate measurements for each standard addition (with typically two additions, but sometimes three). The standard addition method is a form of internal calibration curve, where a small volume of high concentration standard solution is added, allowing the operator to determine the sensitivity of the electrode in each different sample matrix, correcting for interferences. The peak height was used to calculate the original arsenic concentration. Samples with high As levels required dilution (up to 200 times with distilled water) for the peak to fall within the linear range. Voltammetric peaks were usually very well defined, though in some cases a background subtraction procedure was applied. The background subtraction procedure involves performing one voltammetric scan with a very short deposition time (e.g. 1 s), which is subtracted from all analytical scans (sample + standard additions) [28]. After each standard addition, the electrode cell and the electrodes were rinsed with distilled water and left standing in water. When not in use or during transportation, electrodes were stored dry in a plastic container.

The voltammetric cell was 20 mL in volume and analysis was completed under ambient temperature, in the presence of dissolved oxygen. Total As was measured in chloride containing acetate solution (CLAC, 80 mM + 0.25 M NaCl) at pH 4.7 after addition of up to 10 μM KMnO_4 (the novel procedure developed in this work) and in 0.1 M HCl (representing the benchmark procedure [24,28]). The ASV parameters were the same for both electrolytes: a conditioning potential at $+700$ mV for 5 s, followed by a deposition step at -1200 mV for 10–60 s, depending on the required detection limit. After deposition, a 10 s holding potential of -400 mV was applied, followed by a linear sweep from -400 to 800 mV at 8 V s^{-1} (step size of 2 mV, step duration of 250 μs). Arsenic can be detected by a number of voltammetric methods including square wave or differential pulse; here, with the PDV6000 potentiostat, linear sweep voltammetry (LSV) with a stripping scan rate of 8 V s^{-1} was preferred. The current measuring range was set at 100 μA . The solution was continuously stirred (at 250 RPM) during the

conditioning and deposition step, but not during the hold and sweep steps.

All samples collected in India and Mexico were measured both in CLAC and in HCl and the results were compared. Voltammetric analysis in India 2019 was conducted by 2 different operators, one operator running the measurements in CLAC and the other one in HCl. In Mexico in 2021 and in India in 2022, a third operator ran all the measurements.

2.5. Determination of analytical parameters

The linear range was obtained by plotting the change in arsenic peak height as a function of the concentration of As(V) as standard additions of arsenic were added into the electrochemical cell. The sensitivity of the electrode within any given buffer solution/electrolyte was defined by the slope of the linear range and normalised to the deposition time ($\text{nA} \cdot \text{ppb}^{-1} \cdot \text{s}^{-1}$). The detection limit (LoD) was calculated as 3σ , where σ is the standard deviation in the height of the arsenic stripping peak calculated from 10 repeat scans in the presence of a relative low concentration of arsenic (e.g. $0.5 \mu\text{g L}^{-1}$) [44].

2.6. ICP-MS analysis

High Resolution Inductively Coupled Plasma Mass Spectrometer (HR ICP-MS, Element 2, Thermo Finnigan, Bremen) was used for the determination of elemental concentrations including arsenic, iron, copper and manganese. The samples were prepared in pre-cleaned 10 mL polyethylene tubes (Sarstedt). Samples were further acidified with 2% HNO_3 (Carl Roth, ROTIPURAN®Supra). Indium (115) was used as an internal standard and was added to all the samples at a concentration of $10 \mu\text{g L}^{-1}$. Concentrations were determined by means of external 5-point calibration ($0\text{--}100 \mu\text{g L}^{-1}$). No special setup of the instrument operating conditions was needed. Further, quality control (QC) of HR ICP-MS measurements was conducted by the determination of element concentrations in the internal river water standard (previously “calibrated” using “River Water Reference Material for Trace Metals”, SLRS-5, National Research Council Canada). A good agreement with expected values for the SLRS-5 concentrations was obtained for all elements. Analysis of India groundwater samples in 2022 was performed using an Agilent 8900 MS/MS (QQQ) instrument. Similar to the previous batch of analyses, Indium was added as an internal standard ($10 \mu\text{g L}^{-1}$). Elements were measured in “He” (Helium) mode, and Fe and As additionally in “H₂” (Hydrogen) mode to reduce interferences.

2.7. Humic substances analysis by cathodic stripping voltammetry

Groundwater samples from the Indian and Mexican sampling campaign in 2022 and 2021 were analysed for electroactive humic substances using a mercury hanging drop electrode (HDME, Metrohm) and the voltammetric method was adopted from Pernet-Coudrier et al. [54]. Briefly, under a laminar flow hood, aliquots of groundwater (10 mL) were pipetted into an acid-cleaned quartz voltammetric cell. The solution was spiked with $30 \mu\text{L}$ of 10mg L^{-1} Mo (VI), corresponding to an addition of 375nmol L^{-1} . The sample was then acidified to pH 2 with HCl, and purged with N_2 for 300 s. The analytical scan consisted of the application of a deposition potential of 0 V applied for 150 s. The principle here is that the molybdenum will complex with the humic substances, and the complexes are subsequently deposited on the HDME. The stirrer was switched on for the deposition and stopped before a 5 s equilibrium step. Stripping was performed in differential pulse mode, initiated at 0 V and terminated at -0.65 V with a modulation time of 60 ms, a modulation amplitude of 50 mV, a step potential of 2 mV and an interval time of 0.1 s. At the start of the standard addition procedure a background subtraction procedure was applied. The background scan used all parameters the analytical scan except for a 1 s deposition time. This background scan was subtracted from all analytical scans to give background-subtracted scans. The standard addition

procedure consisted of a minimum of four repeat scans for the sample and each of the two standard additions.

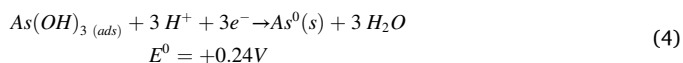
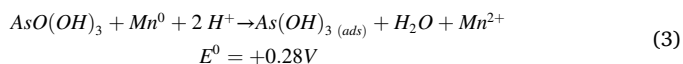
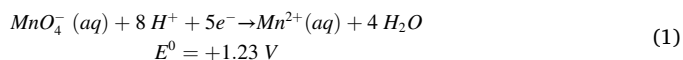
2.8. Scanning electron microscopy

Electron microscopy was performed at the SEM Shared Research Facility, University of Liverpool, to investigate the effect that the repeated measurements over several weeks in groundwater had on the surface of the gold electrodes. Backscattered electron (BSE) images were collected on a Zeiss Gemini 450 FEG-SEM using an accelerating voltage of 20 kV and a probe current of 10 nA.

3. Results and discussion

3.1. Effect of the permanganate concentration

Mn(II) was shown to facilitate the reduction of As(V) to As(0) in seawater (pH 8) [25]. Together with the addition of an oxidant to oxidise any As(III) present to As(V), total inorganic arsenic was detected at this high pH. Here, we decided to test whether permanganate would facilitate the reduction of As(V) since MnO_4^- is a strong oxidant which converts As(III) to As(V) within seconds. The effect of permanganate ($0\text{--}100 \mu\text{M}$) on the detection of $10 \mu\text{g L}^{-1}$ (133nM) As(V) in the CLAC electrolyte is shown in Fig. 2. It is very similar to the effect observed with Mn(II), i.e. a much improved detection of As(V) at low deposition potentials, most certainly due to the reduction of the permanganate anion to Mn^0 at the electrode surface. The optimum KMnO_4 concentration was found to be $10 \mu\text{M}$ when using a -1.2 V deposition potential, however only $2 \mu\text{M}$ permanganate was necessary to yield a significant increase of the As(V) signal. The optimum Mn(II) concentration in these conditions was $3.5 \mu\text{M}$ (Fig. S2). A shift in the optimum deposition potential from -1.25 V to -1.1 V was observed when increasing the KMnO_4 concentration from 0 to $100 \mu\text{M}$. No As(V) signal was obtained at deposition potentials above -1.0 V. The peak height obtained with $10 \mu\text{g L}^{-1}$ As(V) increased by a factor between 4 and 8 (depending on the deposition potential) when KMnO_4 concentrations were increased from 0 to $10 \mu\text{M}$. The peak potential was $+35$ mV, with a peak height of $1.47 \mu\text{A}$ and half-peak width of ~ 66 mV. Similarly to what was described for Mn(II) [25], the various electrochemical and chemical reactions taking place at the electrode during the deposition step at pH 4.7 are summarized by equations (1)–(4) [55,56] where Mn_{ads}^0 and As_{ads}^0 represent the reduced manganese and reduced arsenic that are adsorbed at the gold surface.



3.2. Effect of pH and halogens

Analysis was optimised in buffered conditions to avoid any change of pH due to the reduction of dissolved oxygen. It is known that halogens may affect the intensity and shape of the arsenic signal [23]. The effects of chloride, bromide and iodide on the As(V) peak were tested in buffer solutions at various concentrations and different deposition potentials (Fig. S3). We found that the presence of iodide had the least impact on the As(V) peak height. Bromide increased the peak height, but peaks were generally wider than those obtained in the presence of chloride.

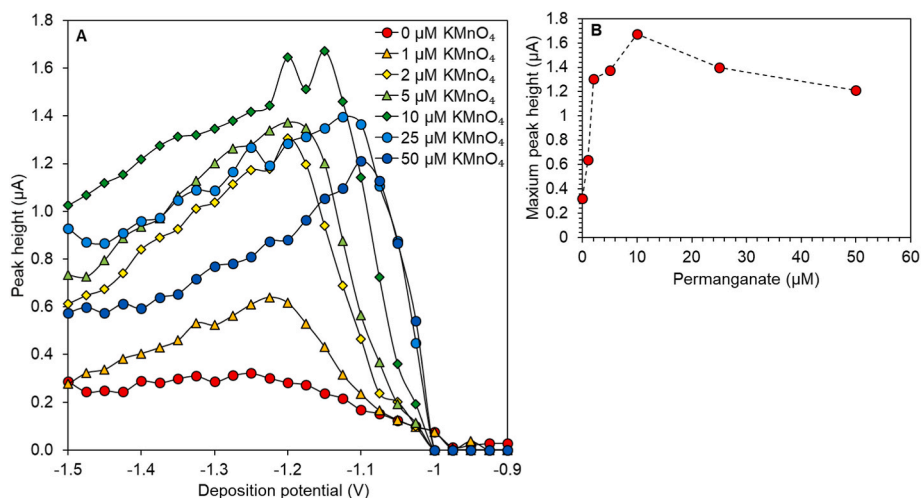


Fig. 2. A: Peak height of $10 \mu\text{g L}^{-1}$ As(V) as a function of KMnO_4 concentration and deposition potential. $t_{\text{dep}} = 10$ s. Electrolyte used was 60 mM acetate, 20 mM acetic acid, and 0.25 M sodium chloride with pH 4.7 (CLAC buffer). B: Maximum peak height as a function of permanganate concentration.

Four different buffer solutions with varying pH were tested in the presence of 2–10 μM KMnO_4 and with/without 0.1 M NaCl. Buffers included: a 10 mM acetate buffer (pH = 4.7), a 10 mM phosphate buffer (pH = 7), 10 mM TES (pH = 7.8), and 10 mM borate buffer (pH = 9). The presence of permanganate facilitated the detection of As(V) in all buffers tested, and the arsenic peak was always enhanced by the addition of 0.1 M NaCl in all buffer solutions (Fig. 3). The presence of 0.1 M NaCl resulted in an increase in As(V) peak height by a factor 2.00 in 10 mM acetate, by a factor of 1.54, 1.58, and 2.58 in 10 mM phosphate, TES, and borate respectively. The peak position shifted cathodically (to more negative potentials) as pH increased (at approximately the Nernstian predicted shift of 56 mV/log pH) [27,46] but was also affected by the presence of chloride, although this effect was different for each buffer.

3.3. Analytical parameters

The analytical parameters (linear range, limit of detection, and sensitivity) and peak characteristics (peak potential, peak half-width) were measured for each buffer in the absence/presence of 0.1 M chloride and at various deposition times (Table 1). Table 1 also includes data for 0.1 M HCl electrolyte and the CLAC buffer (80 mM acetate + 0.25 M NaCl) which is the electrolyte used in all fieldwork experiments reported thereafter. Selected voltammograms in the presence of chloride are shown in Fig. 4 for each buffer solution. The linear range was inversely

correlated to the deposition time and, in general, inversely correlated to sensitivity [28]. The presence of chloride generally sharpens the As peak (i.e. decreased the peak width) while keeping a similar sensitivity; it also increased the linear range. The optimum response (highest sensitivity, sharpest peak, and widest linear range) was obtained in the CLAC buffer, with detection limits of $0.28 \mu\text{g L}^{-1}$ and $0.14 \mu\text{g L}^{-1}$ for 10 s and 30 s deposition times respectively (Fig. 4c and d). The response was not as analytically favourable in 0.1 M HCl as in CLAC (lower sensitivity, slightly wider peak) resulting in almost twice higher detection limits at the same deposition times. In comparison to methods used in other studies (Table S3), these analytical parameters are satisfactory, especially considering the short deposition time used, non-acidic pH conditions, and the use of a non-modified electrode that can be used for hundreds of analyses.

The sensitivity obtained with the CLAC buffer is significantly higher than in 0.1 M HCl showing that the reduction of As(V) as facilitated by reduced manganese (Eq. (4)) is more efficient than the effect of nascent hydrogen on As(V) reduction. However, while the sensitivity obtained in HCl was largely independent of the deposition time, that was not the case for the other buffers, apart from borate (Table 1). For instance, in the CLAC buffer, the sensitivity (normalised to the deposition time) decreased from 63.5, 55.5 to $44.4 \text{ nA ppb}^{-1} \cdot \text{s}^{-1}$ for deposition time of 10 s, 30 s and 60 s respectively, suggesting some progressive adsorption of the sodium, acetate and/or chloride at the deposition potential used

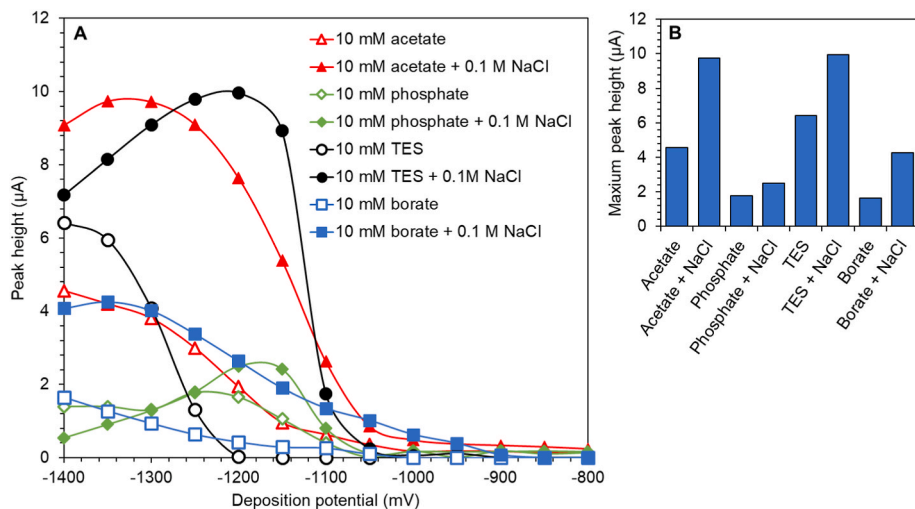


Fig. 3. A: Scanned stripping voltammetry of As(V) peak height at different pH in the absence/presence of 0.1 M NaCl, $t_{\text{dep}} = 30$ s, $2 \mu\text{M}$ KMnO_4 , $10 \mu\text{g L}^{-1}$ As(V), 25 μm gold microwire. Red = 10 mM acetate buffer (pH = 4.7); grey = 10 mM phosphate buffer (pH = 7); black = 10 mM TES buffer (pH = 7.8); blue = 10 mM borate buffer (pH = 9). Filled circles indicate the presence of 0.1 M NaCl and open circles indicate no NaCl. B: maximum peak height measured in the different electrolytes. (For interpretation of the references to colour in this figure legend, the reader is referred to the Web version of this article.)

Table 1

Analytical parameters at varying pH; All peak data were obtained with 30s deposition time in the presence of 10 $\mu\text{g L}^{-1}$ As(V) using linear scan stripping (8 V s^{-1}). Note that the sensitivity is normalised to the deposition time. *: Experiments carried out with electrode 1; **: Experiments carried out with electrode 2.

Solution	pH	Optimal deposition potential (V)	Peak potential (mV)	Peak height (μA)	Peak half width (mV)	Peak height/Peak half width ($\mu\text{A/V}$)	$t_{\text{dep}} = 10$ s Linear range ($\mu\text{g L}^{-1}$); Sensitivity ($\text{nA.ppb}^{-1}.\text{s}^{-1}$); Limit of detection ($\mu\text{g L}^{-1}$)	$t_{\text{dep}} = 30$ s - Linear range ($\mu\text{g L}^{-1}$); Sensitivity ($\text{nA.ppb}^{-1}.\text{s}^{-1}$); Limit of detection ($\mu\text{g L}^{-1}$)	$t_{\text{dep}} = 60$ s - Linear range ($\mu\text{g L}^{-1}$); Sensitivity ($\text{nA.ppb}^{-1}.\text{s}^{-1}$); Limit of detection ($\mu\text{g L}^{-1}$)
0.1 M HCl*	1.0	-1.2	141	8.5	120	71	≤ 20	≤ 8	≤ 4
							31	36	30
							0.50	0.23	0.07
80 mM acetate + 0.25 M NaCl (CLAC)*	4.7	-1.2	7	16.0	108	148	≤ 20	≤ 10	≤ 5
							64	55	44
							0.28	0.14	0.07
10 mM acetic acid**	4.7	-1.4	37	7.1	136	52	≤ 10	≤ 5	≤ 2
							40	30	36
							0.60	n.d.	0.12
10 mM acetic acid +0.1 M NaCl**	4.7	-1.4	-50	10.1	140	72	≤ 20	≤ 6	≤ 4
							44	39	36
							0.50	0.38	0.11
10 mM phosphate**	7.0	-1.2	-117	1.0	182	5.5	≤ 10	≤ 10	≤ 2
							9.5	3.8	5.4
							n.d.	n.d.	n.d.
10 mM phosphate +0.1 M NaCl**	7.0	-1.2	-113	1.6	120	13	≤ 50	≤ 50	≤ 15
							7.5	4.9	4.2
							n.d.	n.d.	n.d.
10 mM TES**	7.8	-1.4	-97	4.8	160	30	≤ 4	≤ 6	≤ 4
							28	21	16
							0.95	0.51	0.27
10 mM TES +0.1 M NaCl**	7.8	-1.2	-115	6.2	144	43	≤ 20	≤ 10	≤ 4
							23	22	25
							0.88	0.46	0.17
10 mM borate**	9.0	-1.4	-356	1.7	134	13	≤ 20	≤ 8	≤ 8
							6.0	6.7	5.2
							n.d.	n.d.	n.d.
10 mM borate +0.1 M NaCl**	9.0	-1.35	-355	3.1	232	13	≤ 20	≤ 10	≤ 8
							10	11	9.9
							2.01	0.94	0.60

(-1.2 V). Adsorption in 0.1 M HCl is probably less due to the immediate reduction of the proton at this low deposition potential.

The sensitivities obtained in the phosphate buffer (Fig. 4e and f) and borate buffer (Fig. 4i and j) were relatively low compared to that obtained in acetate solution. However, in the phosphate buffer, the linear range was significantly higher (2.5 times higher than in CLAC, up to 50 $\mu\text{g L}^{-1}$ for 10 s deposition). A relatively small linear range for As detection has often been reported and is attributed to the saturation of the electrode with non-conductive As(0), preventing further deposition [28]. The sensitivity obtained in 10 mM TES buffer (Fig. 4g and h) was less than half of that obtained in CLAC, even though the signal was well shaped. Electrode stability was tested by performing 30 scans in CLAC and HCl solution in presence of 10 ppb As(V) ($E_{\text{dep}} = -1200$ mV; $t_{\text{dep}} = 10$ s). Peaks were stable and reproducible in both solutions: the standard deviation in As peak height over 30 scans in CLAC was 2.9% and 2.7% in 0.1 M HCl. In CLAC, peak height increased linearly with scan rate, as expected for adsorbed species at the surface of a solid electrode. The experiments carried out in 0.1 M acetate/TES/borate or phosphate with/without 0.1 M NaCl were done with the same electrode at a similar time (absolute sensitivities can thus be compared), while the experiments carried out in CLAC and in HCl were done with a different electrode at a different time. Comparisons of absolute sensitivities obtained by these different electrodes should be done with caution as we found that the electrode history impacts those sensitivities; for instance, using a new electrode, only slight differences (10%) were obtained between CLAC and 10 mM acetate + 0.1 M chloride solution, much less than the 35% difference given in Table 1. Nevertheless, best signal sensitivities were constantly found in CLAC, which was used as our optimum

electrolyte.

3.4. Interferences of metals and organic matter

We identified that CLAC + KMnO_4 gave the best performance among all the near neutral pH buffers tested, even better than the benchmark HCl method. Because of these obtained results, we chose to go forward testing and validating CLAC + KMnO_4 as a substitute to the HCl method. The presence of other metals and humic substances on the As signal was tested in CLAC + 10 μM KMnO_4 and compared to their effect in 0.1 M HCl. Concentrations of these possible interferences were kept at environmentally relevant levels.

3.4.1. Copper interference

Copper is well-known to interfere with arsenic detection in acidic conditions due to both peak potentials being relatively close to one another at pH 1 (+0.3 V and +0.1 V respectively) [57]. When increasing the pH from 1 to 4.7 (using the CLAC + KMnO_4 solution), the As peak shifts cathodically from +0.11 V to 0 V while the Cu peak potential remains relatively unchanged (+0.35 V), giving a larger peak separation of c. a. +0.35 V. In agreement with previously reported results [25], we found that this increased peak separation resulted in less interference from copper. For instance, in 0.1 M HCl, the signal of 1 $\mu\text{g L}^{-1}$ As(V) was completely lost after the addition of just 16 $\mu\text{g L}^{-1}$ Cu, while in CLAC method, the As peak could be distinguishable until the addition of 32 $\mu\text{g L}^{-1}$ Cu (Fig. 5a). The same pattern was observed for a higher concentration of 10 $\mu\text{g L}^{-1}$ As(V). Copper concentrations are usually around 0.1–50 $\mu\text{g L}^{-1}$ in groundwaters investigated in this study, where any

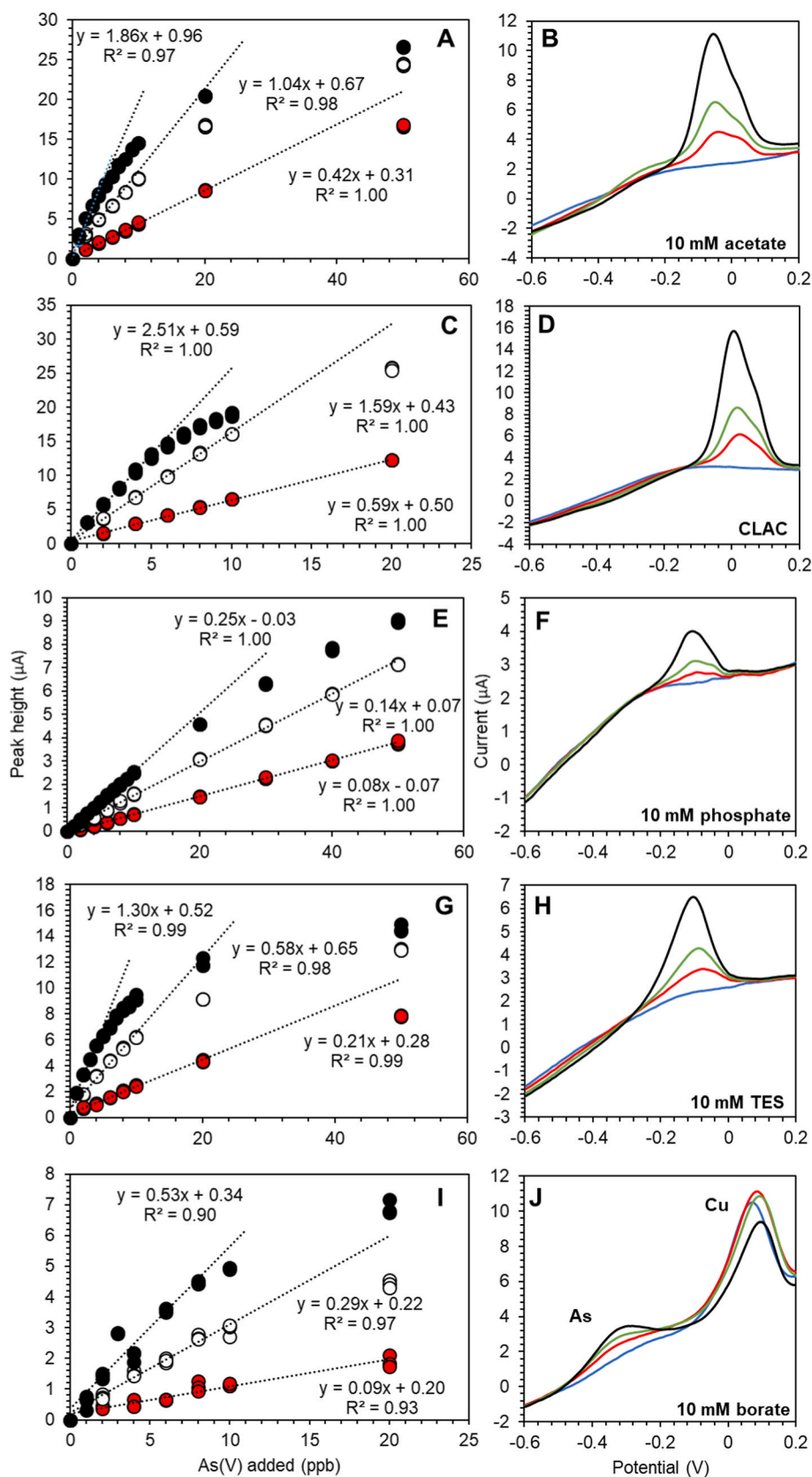


Fig. 4. Calibration curves and voltammograms for 0.1 M chloride containing 10 mM acetate (A and B respectively), CLAC (C and D), 10 mM phosphate (E and F), 10 mM TES (G and H), 10 mM borate (I and J). Red circles: $t_{\text{dep}} = 10\text{s}$; white circles: $t_{\text{dep}} = 30\text{s}$; black circles: $t_{\text{dep}} = 60\text{s}$. Using optimal E_{dep} as shown in Table 1, 25 μm gold microwire, and 2 μM KMnO_4 . Voltammograms shown were done with $t_{\text{dep}} = 10\text{s}$. Black line = 20 $\mu\text{g L}^{-1}$ As(V); green line = 8 $\mu\text{g L}^{-1}$ As(V); red line = 4 $\mu\text{g L}^{-1}$ As(V); blue line = 0 $\mu\text{g L}^{-1}$ As(V). (For interpretation of the references to colour in this figure legend, the reader is referred to the Web version of this article.)

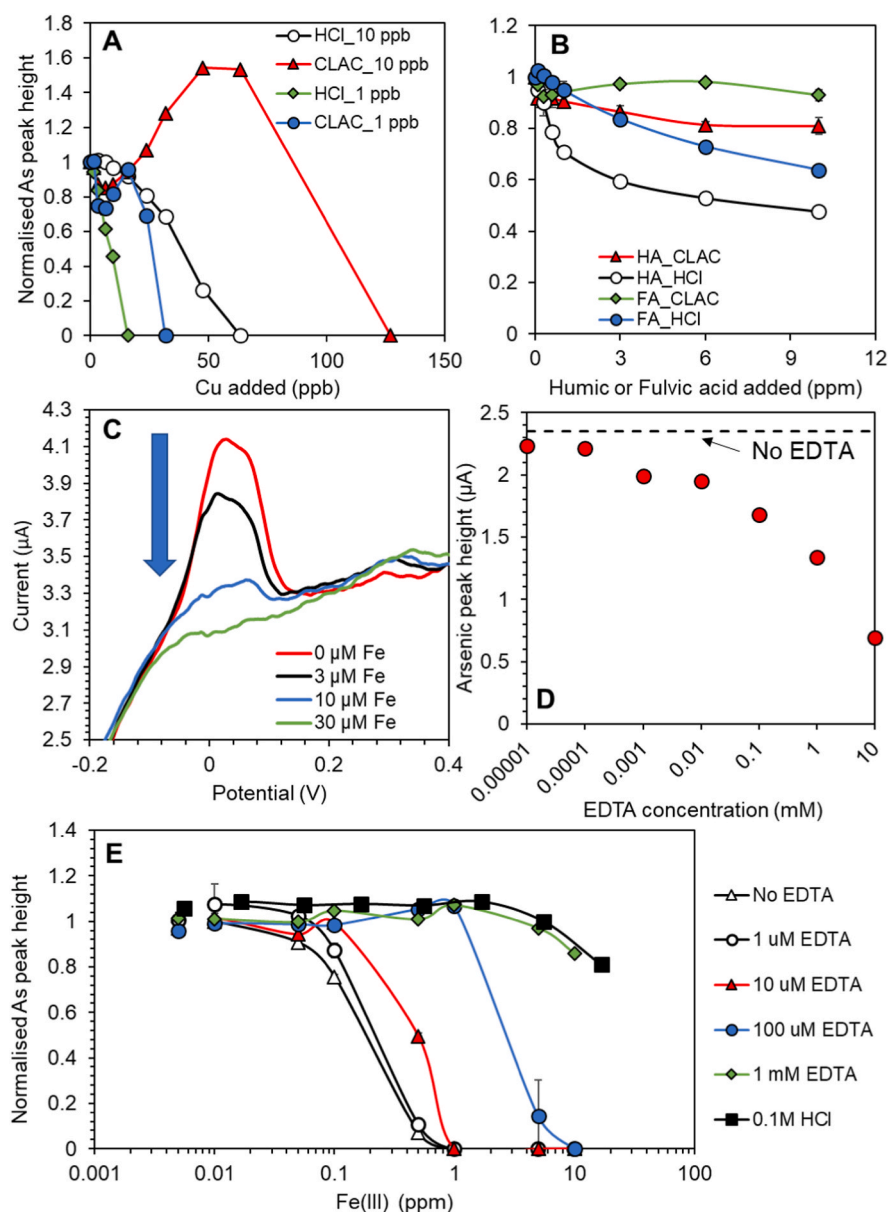


Fig. 5. A: effect of copper; B: effect of humic and fulvic acid; C: Voltammogram showing As(V) peak decrease as a function of Fe(III) in CLAC (no EDTA); D: effect of EDTA on As(V) peak in CLAC; E: effect of Fe(III) on As(V) peak in the presence of EDTA. All experiments were performed with 25 μm gold microwire electrode, 10 $\mu\text{g L}^{-1}$ As(V), $E_{\text{dep}} = -1200$ mV, $t_{\text{dep}} = 10$ s, and 10 μM KMnO_4 . Points in figures are averages of triplicate measurements and standard deviations are given as error bars. (For interpretation of the references to colour in this figure legend, the reader is referred to the Web version of this article.)

interference observed using the benchmark HCl method is unlikely to be also seen using the new CLAC + KMnO_4 method. In case of samples containing much higher copper concentrations, a complexing agent could be used (though not EDTA, since the deposition potential of -1.2 V will pull the copper out of the EDTA-complex).

3.4.2. Humic and fulvic acid interference

Groundwater dissolved organic carbon contents typically range between 0.1 and 15 mg L^{-1} . In this work, dissolved organic carbon was represented using humic acid (HA) and fulvic acid (FA), and the influence of these upon As detection using both benchmark HCl and the new CLAC + KMnO_4 methods was investigated. The presence of 10 mg L^{-1} humic acid decreased the As(V) peak height both in 0.1 M HCl and in CLAC but the effect was much weaker in CLAC (20% loss compared to 50% in 0.1 M HCl) (Fig. 5b). Similarly, the presence of 10 mg L^{-1} fulvic acid resulted in only 7% decrease in peak height for As(V) in CLAC solution, as compared to a 26% decrease in acidic conditions (see Fig. 5b). An anodic peak shift was observed in both electrolytes as HA and FA concentrations increased. However, the arsenic peak is still clearly visible and the standard addition method can still be applied. The

decrease in peak intensity observed in the presence of HA and FA might be due to their adsorption onto the gold microwire [58], although As(V) complexation with humic substances could also play a role [59]. The results indicate that the CLAC + KMnO_4 method is more robust towards the presence of high dissolved organic carbon contents as compared to the benchmark 0.1 M HCl method.

3.4.3. As(V) detection in Fe(III) and Mn(II) containing solutions

Groundwaters may contain concentrations of Fe(II) and Mn(II) in excess of 500 μM [16], and both ions are known to precipitate with As(V) at neutral pH under oxidising conditions [60]. The effect of Fe(III) and Mn(II) on the As(V) sensitivity on the gold microwire was tested in laboratory conditions by successively increasing Fe(III) and Mn(II) concentrations. The results are presented in Fig. 5c. In 0.1 M HCl, the presence of Fe up to 10 mg L^{-1} did not affect the As(V) signal (Fig. 5e). In contrast, in CLAC, the As(V) peak height decreased rapidly as Fe concentration increased, with a complete loss at 30 μM Fe (1.67 mg L^{-1}) (Fig. 5c). The decrease in arsenic signal might be attributed to removal of As(V) from the dissolved phase by adsorption onto newly precipitated iron oxyhydroxides [61], which does not occur at pH 1 (0.1 M HCl). This

is a clear difference between the two pH levels and may be advantageous as it would allow the user to measure the truly dissolved (non-adsorbed) inorganic arsenic at high pH, and the total inorganic arsenic (dissolved + adsorbed) in acidic conditions, where the low pH will cause desorption of arsenic, similar to results reported in estuarine waters [51]. Nevertheless, this experiment further strengthens the importance of rapid analysis of groundwater and avoiding the formation of oxide species after the sampling of water that would eventually change As speciation. This is particularly important for reducing groundwater conditions such as India, which tend to contain high levels of iron [16], which readily oxidises and precipitates once in contact with air.

Previous studies have shown that addition of acid or EDTA immediately after sample filtration are effective in preventing precipitation of such iron oxide/hydroxides and thereby changing arsenic speciation

[16]. Here, we tested the effect of EDTA on the detection of As(V) in CLAC in the presence of 10 μM KMnO_4 with/without high levels of Fe (III). The As(V) signal decreased as the EDTA concentration increased (Fig. 5d), possibly due to the complexation of Mn(II) with EDTA, inhibiting its electrochemical reduction at the electrode surface (Eq. (2)). Whilst the peak height decreased (40% lower at 1 mM EDTA), the position and shape of the As(V) peak was not significantly altered. Addition of 1 mM EDTA in CLAC, allowed the detection of As(V) even in the presence of high Fe(III) concentrations of 180 μM (10 mg L^{-1}) (Fig. 5e).

In West Bengal, concentrations of 45 μM Mn have been reported in groundwater [16]. We tested the effect of Mn(II) concentrations up to 300 μM (16 mg L^{-1}) on the arsenic signal. In both acidic and near-neutral electrolytes, no significant effect was observed (Fig. S4).

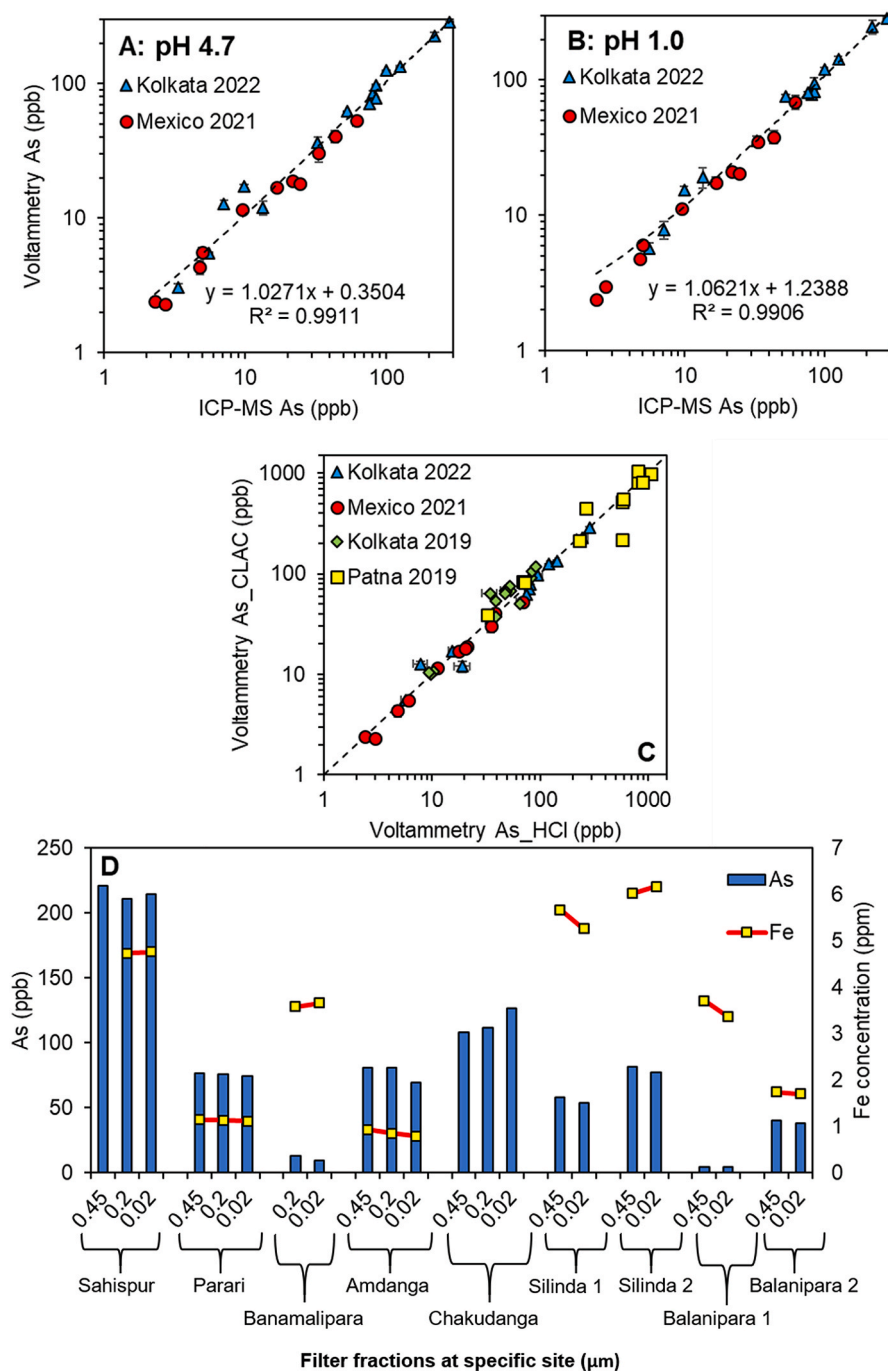


Fig. 6. A and B = Inorganic arsenic measurements in CLAC and 0.1 M HCl respectively by voltammetry vs. ICP-MS measurements in Kolkata (2022) and Mexico (2021). C = All arsenic measurements analysed by voltammetry during this study. D = Inorganic arsenic concentration measured by ICP-MS as a function of filter fractions at nine different stations in West Bengal, plotted with the iron concentration at those specific sites. Points in figures are averages of triplicate measurements and standard deviations are given as error bars.

3.5. Field analysis

3.5.1. Total inorganic arsenic determination

The groundwater samples collected in Mexico had arsenic concentrations varying from 1 to 90 $\mu\text{g L}^{-1}$, while concentrations in India varied from 3.4 to 1157 $\mu\text{g L}^{-1}$, the highest concentrations being detected in Chapar, Bihar. For both countries, total inorganic As concentrations determined by voltammetry in the CLAC buffer (pH 4.7) and in HCl (0.1 M) agreed very well with ICP-MS measurements (with slopes of $+1.03 \pm 0.02$, $R^2 = 0.99$ and $+1.06 \pm 0.02$, $R^2 = 0.99$ respectively, Fig. 6a and b). These measurements include eight groundwater wells and three treated drinking water sources in Mexico, and fifteen groundwater wells in Chakdaha block (West Bengal). The samples were collected at various depths (Table S1), from shallow (~ 15 m) to deep aquifers (~ 150 m) with varying chemical compositions (Table 2). For all samples, the concentration measured by voltammetry in CLAC provides a very good estimate of the total arsenic concentration, as measured by ICP-MS (Fig. 6a). Good correlation was also found between voltammetric measurements done in CLAC and in HCl (Fig. 6c), although variation was observed in samples collected in India 2019. This variation may be an artefact of data recording, because two different operators were running the measurements. Considering all data, the correlation between concentrations in CLAC and HCl is strong (slope 0.95 ± 0.04 , $R^2 = 0.93$, Fig. 6c) but improves substantially if samples from India 2019 are discarded, and only those from India 2021 and Mexico 2022, where only one operator ran all sampling, are included in the analysis (slope = 0.96 ± 0.02 , $R^2 = 0.99$). The good agreement between voltammetry and ICP-MS for all groundwaters samples tested here indicates that all arsenic was present in a voltammetrically labile form, i.e. as inorganic species, since unlike ICP-MS analysis of acidified samples, voltammetric techniques are not sensitive to the presence of organic arsenic (e.g. DMA [27]).

Humic substances have been shown to interfere with the As(V) signal in both 0.1 M HCl and in the CLAC buffer at concentrations in the range of 0.5 mg L^{-1} to 10 mg L^{-1} in laboratory conditions (section 3.4.2). No interference was observed during analysis, due to the high dilution factors. Mexican groundwater samples all had relatively low humic concentrations ($<20 \mu\text{g L}^{-1}$, Table 2) while groundwaters in West Bengal had relatively high levels of humic concentration, between 0.5 and 1.3 mg L^{-1} . Whilst arsenic can be complexed by organic matter [51, 59], such as humic and fulvic acids present in reducing Indian groundwaters, the agreement between ICP-MS and CLAC + KMnO_4 detection at pH 4.7 indicates that any such complexes would have been voltammetrically labile.

3.5.2. Effect of filter sizes on As concentration

During the sampling campaign in India in 2019, groundwater wells were filtered with 0.45, 0.2, and 0.02 μm membrane filters immediately after collection. The 0.02 μm filtering was done using the 0.45 μm filtrate to avoid possible blockage of the filter. Filtration was done within 10 min of sampling. All these samples were analysed by ICP-MS. Interestingly, there were no significant differences in dissolved As and Fe concentrations in the filtrate of the 0.45, 0.2 and 0.02 μm filters, indicating that (1) arsenic is present in the soluble fraction, and (2) precipitation of iron was not significant in any of those samples within the short time that the water filtering was performed (Fig. 6d). This experiment suggests that filtration can be performed immediately after sampling, before the precipitation of iron oxides occurs, without altering the arsenic speciation. Similar experiments were done in Mexico with the addition of an unfiltered sample measured by ICP-MS. Likewise, no significant differences in arsenic concentration were found as a function of the filter size (Fig. S5).

3.5.3. Electrode stability during field campaigns

We used microwire electrodes fabricated using a new method. It was important to assess the stability, robustness, and reproducibility of these

electrodes. The same type of working electrodes (Gold WireBond) were used for the three fieldwork campaigns; in Mexico 2021 and India 2022, only one electrode was used for each fieldwork; in India 2019, different electrodes were used in CLAC and HCl. The stability of the electrode was assessed by (1) monitoring the gold oxide reduction peak in 0.5 M H_2SO_4 (which is directly proportional to the real surface area of the electrode [52]); (2) monitoring the electrode sensitivity as given by the slope of the standard additions; (3) collecting backscattered electron (BSE) micrographs of the electrode used in India 2022 before and after use.

Firstly, the gold oxide reduction peak remained stable over the course of the fieldwork in Mexico 2021 and India 2022. This observation did not agree with the decrease in electrode sensitivity that was measured during analysis. This decrease in sensitivity was related to the increased usage (i.e. decrease in sensitivity with increased usage). If there were no interferences, and assuming reproducible stirring conditions and constant chemical conditions (e.g. concentrations of acid or EDTA), the sensitivity should remain constant for the same type of electrode (i.e. 25 or 30 μm diameter). This was not the case and significant variations in sensitivity were observed during analysis in India (Table 2), similar to results in another study where arsenic analysis was performed under acidic conditions [24]. BSE images (Fig. 7) of the electrode used in India 2022, for measurements in both CLAC and HCl, show increased roughness of the electrode surface, although no increase in the size of the gold oxide reduction peak was observed during the conditioning of the electrode. Surprisingly, when scanning the electrode, we observed a layer peeling off the surface. The thin layer (estimated thickness of approximately 0.2 μm) contains numerous, mostly circular holes. Energy dispersive X-ray spectroscopy (EDX) identified the composition of the layer to be gold, suggesting that the layer peeled away from the surface is the gold microwire itself (Fig. S6). Hydrogen bubbles may be responsible for the presence of the circular holes observed in the peeled layer, produced either during the sulfuric acid cleaning stage or during analysis in 0.1 M HCl. Further work is required to determine whether hydrogen is responsible for the observed surface damage, however, these observations indicate that hydrogen generation at the gold electrode may not be beneficial to the mechanical stability of the electrode. Because strong hydrogen generation is used for the cleaning process in sulfuric acid (-2 V for 10 s) for all electrodes, this might explain why similar loss of sensitivity with usage is observed for measurements carried out in 0.1 M HCl or in CLAC.

The sensitivity, as measured by the slope of standard additions, varied considerably from 60 to 70 $\text{nA ppb}^{-1} \cdot \text{s}^{-1}$ to below 10 $\text{nA ppb}^{-1} \cdot \text{s}^{-1}$. Such variations are large and unexpected. We checked how the sensitivity varied with age of the electrode, deposition time, dilution factor, concentrations of humic substances, EDTA, Fe, Mn or Cu in the voltammetric cell (Table S2 and Fig. S7). The main influencing factor for the decrease in sensitivity seems to be electrode usage. A high dilution factor tends to increase the sensitivity, suggesting an interference effect from the species present in the groundwater. Interestingly, there does not seem to be much difference between the decrease of sensitivity observed in CLAC and in HCl (Figure S7 H-J), suggesting that acidic conditions are not responsible for the observed changes and measuring at a higher pH does not improve the stability of the sensitivity. We tested the effect of imposing +800 mV (highest potential used in our procedure) in CLAC by running 1000 stripping scans preceded by 5s at 800 mV. An increase of the roughness was clearly visible on SEM pictures compared to an electrode having gone through the same treatment but up to 500 mV only (Fig. S7). However, it is likely that the change in electrode sensitivity is due to a combination of factors, including memory effects, composition of the water tested, efficiency of the cleaning stage (in sulfuric acid), deposition time, and age of the electrode. In any case, such variation in sensitivity shows that arsenic concentrations can only be determined through the method of standard addition; an external calibration procedure would result in significant errors.

Table 2
 Voltammetric and ICP-MS measurements in West Bengal (WB1 = 2019; WB2 = 2022), Bihar (B) and Central Mexico (Mex). n.d = not determined; n.a. = not available anymore. The uncertainty given is the standard deviation of triplicate measurements.

Site Information		Voltammetric measurements							ICP-MS measurements				
Site	Total As _{CLAC} ($\mu\text{g L}^{-1}$)	Sensitivity (nA. $\text{ppb}^{-1}\cdot\text{s}^{-1}$)	Dilution factor	Deposition time(s)	Total As _{HCl} ($\mu\text{g L}^{-1}$)	Sensitivity (nA. $\text{ppb}^{-1}\cdot\text{s}^{-1}$)	Dilution factor	Deposition time(s)	Humic substances ($\mu\text{g L}^{-1}$)	As ($\mu\text{g L}^{-1}$)	Fe ($\mu\text{g L}^{-1}$)	Mn ($\mu\text{g L}^{-1}$)	Cu ($\mu\text{g L}^{-1}$)
Caminos land (Mex)	16.9 ± 1.3	20	10	30	17.6 ± 1.5	23	10	30	n.d.	16.1	8.5	0.3	1.7
San Luis Rey (Mex)	11.5 ± 0.6	9.6	4.0	30	11.3 ± 0.8	17	1.1	10	9.0 ± 0.4	9.4	23.4	6.9	2.5
Puerto de Nieto (Mex)	40.4 ± 4.2	13	10	30	38.0 ± 4.3	22	10	30	11.6 ± 1.4	35.5	202.0	20.2	0.2
Sosnabar (Mex)	2.4 ± 0.1	7.3	1.1	60	2.4 ± 0.1	8.4	1.1	60	n.d.	2.3	1.1	0.1	1.1
La Esperanza (Mex)	18.9 ± 1.0	9.9	4.0	30	21.0 ± 1.4	12	1.1	10	13.5 ± 1.2	21.7	3.3	0.3	1.3
Lourdes (Mex)	18.2 ± 0.2	12	4.0	30	20.4 ± 0.7	16	4.0	30	11.4 ± 0.8	24.6	686.1	4.0	0.2
Pozo Hondo (Mex)	30.5 ± 4.4	12	4.0	30	35.3 ± 2.1	13	4.0	30	11.2 ± 0.6	33.3	7.2	0.5	0.3
Ex Hacienda de Jesus (Mex)	52.8 ± 4.1	13	10	30	68.9 ± 8.0	14	10	30	16.0 ± 0.6	61.7	4.9	1.3	1.7
Clyva (Mex)	4.3 ± 0.5	15	1.1	30	4.8 ± 0.2	17	1.1	30	n.d.	4.8	24.6	1.0	2.3
Inmaculada (Mex)	5.6 ± 0.5	14	1.1	30	6.1 ± 0.2	14	1.1	30	n.d.	5.0	18.0	0.9	2.4
Agua Puri (Mex)	2.3 ± 0.1	13	1.1	30	3.0 ± 0.1	16	1.1	30	n.d.	2.7	13.0	0.9	3.1
Silinda 1 (WB2)	85.4 ± 0.9	25	40	10	77.9 ± 3.0	20	20	10	391.5 ± 14.7	80.7	1271.9	88.5	0.2
Silinda 2 (WB2)	77.8 ± 5.6	24	40	10	81.9 ± 0.2	18	20	10	825.1 ± 27	84.4	6080.0	248.1	49.1
Darapur 1 (WB2)	70.4 ± 3.3	22	40	10	80.4 ± 2.2	16	20	10	243.9 ± 10.7	76.3	2701.9	128.5	0.1
Darapur 2 (WB2)	96.8 ± 6.3	23	40	10	94.5 ± 10.0	16	20	10	714.0 ± 22.5	84.5	3042.9	264.5	3.8
Sahispur 1 (WB2)	226.2 ± 19.6	8.3	40	30	246.3 ± 29.2	19	40	10	739.5 ± 16.2	220.5	3924.0	275.4	0.1
Sahispur 2 (WB2)	3.0 ± 0.2	21	1.1	10	n.d.	n.d.	n.d.	n.d.	223.7 ± 8.5	3.4	30.1	130.9	1.1
Sahispur 3 (WB2)	284.3 ± 9.4	9.3	40	30	286.1 ± 5.0	20	40	10	474.9 ± 13.6	280.8	4.6	229.8	0.0
Sahispur 4 (WB2)	62.1 ± 1.0	11	40	30	75.4 ± 2.8	24	40	10	509.7 ± 27.0	52.7	3887.4	140.1	0.3
Banamalipara 1 (WB2)	12.0 ± 0.6	10	4.0	30	19.2 ± 3.3	9.0	4.0	30	242.6 ± 21.3	13.4	2413.8	316.3	12.9
Chakudanga 1 (WB2)	124.5 ± 18.1	13	40	30	120.0 ± 4.6	23	40	30	1172.2 ± 41.0	100.06	4293.4	472.5	1.3
Chakudanga 2 (WB2)	132.8 ± 9.9	11	40	30	143.2 ± 5.9	23	40	10	514.1 ± 22.0	125.8	3109.1	428.8	0.9
Banamalipara 2 (WB2)	5.5 ± 0.2	11	4.0	30	5.7 ± 0.6	13	2.0	30	116.7 ± 2.2	5.5	2.7	473.9	0.1
Banamalipara 3 (WB2)	36.2 ± 0.3	12	10	30	35.6 ± 2.6	5.3	10	30	145.8 ± 19.1	32.8	4977.0	105.7	0.2
Banamalipara 4 (WB2)	12.8 ± 0.7	11	10	30	7.9 ± 1.2	9.3	2.0	30	150.9 ± 4.4	7.1	4857.1	520.9	4.7
Banamalipara 5 (WB2)	17.2 ± 2.9	12	10	30	15.4 ± 1.2	20	10	30	391.3 ± 22.1	9.9	1899.5	332.8	2.1
Sahispur (WB1)	166.8 ± 1.7	87	203	16	137.1 ± 6.5	50	40	10	n.d.	220.8	4730.6	243.3	n.d.
Parari (WB1)	64.0 ± 1.3	79	102	16	36.7 ± 3.0	67	40	10	n.d.	76.5	1144.0	39.3	n.d.
Banamalipara (WB1)	10.6 ± 0.1	78	21	16	10.5 ± 0.6	57	4.0	15	n.d.	12.8	3607.2	311.7	n.d.
Amdanga (WB1)	67.2 ± 0.7	78	102	16	54.0 ± 1.6	64	10	10	n.d.	80.9	852.6	24.6	n.d.
Chakudanga (WB1)	90.7 ± 1.6	65	102	16	83.0 ± 1.9	51	20	10	n.d.	n.d.	8569.3	311.6	n.d.
Silinda 1 (WB1)	37.6 ± 0.6	39	41	16	39.3 ± 1.9	46	20	10	n.d.	54.1	4744.3	83.8	n.d.
Silinda 2 (WB1)	63.4 ± 0.9	29	52	16	47.3 ± 0.6	48	10	10	n.d.	81.4	6224.8	233.3	n.d.
Balinapara 1 (WB1)	3.6 ± 0.4	47	5.0	16	n.d.	n.d.	n.d.	n.d.	n.d.	4.8	3872.4	506.2	n.d.
Balinapara 2 (WB1)	41.7 ± 2.6	36	21	16	49.2 ± 3.4	42	10	10	n.d.	40.5	1743.9	79.9	n.d.
Station 1_Patna (B)	521.4 ± 45.4	n.a.a.	n.a.a.	n.a.a.	571.3 ± 45.4	24	200	10	n.d.	557.0	4014.0	794.4	n.d.
Station 2_Patna (B)	805.5 ± 34.8	n.a.a.	n.a.a.	n.a.a.	809.0 ± 34.8	227	100	5	n.d.	918.7	1716.7	1166.3	n.d.
Station 3_Patna (B)	975.1 ± 63.5	n.a.a.	n.a.a.	n.a.a.	1062.1 ± 63.5	24	100	5	n.d.	1157.1	3256.9	1240.2	n.d.
Station 4_Patna (B)	39.0 ± 2.5	n.a.a.	n.a.a.	n.a.a.	32.4 ± 2.5	14	20	30	n.d.	33.4	66.2	1026.4	n.d.

(continued on next page)

Table 2 (continued)

Site Information	Voltammetric measurements						ICP-MS measurements						
	Total As _{CLAC} ($\mu\text{g L}^{-1}$)	Sensitivity (nA, $\text{ppb}^{-1}\cdot\text{s}^{-1}$)	Dilution factor	Deposition time(s)	Total As _{HCl} ($\mu\text{g L}^{-1}$)	Sensitivity (nA, $\text{ppb}^{-1}\cdot\text{s}^{-1}$)	Dilution factor	Deposition time(s)	Humic substances ($\mu\text{g L}^{-1}$)	As ($\mu\text{g L}^{-1}$)	Fe ($\mu\text{g L}^{-1}$)	Mn ($\mu\text{g L}^{-1}$)	Cu ($\mu\text{g L}^{-1}$)
Station 5_Patna (B)	82.9 ± 4.8	n.a.a.	n.a.a.	n.a.a.	68.7 ± 4.8	17	100	30	n.d.	91.5	207.7	719.9	n.d.
Station 6_Patna (B)	n.d.	n.a.a.	n.a.a.	n.a.a.	18.6 ± 0.8	22	10	20	n.d.	n.d.	n.d.	n.d.	n.d.
Station 7_Patna (B)	211.1 ± 11.9	n.a.a.	n.a.a.	n.a.a.	230.6 ± 11.9	18	40	10	n.d.	223.9	2432.3	524.0	n.d.
Station 8_Patna (B)	1046 ± 26.5	n.a.a.	n.a.a.	n.a.a.	806.2 ± 26.5	25	100	5	n.d.	1086.3	5365.1	527.0	n.d.
Station 9_Patna (B)	552.5 ± 20.9	n.a.a.	n.a.a.	n.a.a.	584.5 ± 20.9	18	100	10	n.d.	614.2	4869.0	1167.5	n.d.
Station 10_Patna (B)	n.d.	n.a.a.	n.a.a.	n.a.a.	16.2 ± 0.8	22	10	15	n.d.	n.d.	n.d.	n.d.	n.d.
Station 11_Patna (B)	447.9 ± 12.2	n.a.a.	n.a.a.	n.a.a.	264.5 ± 12.2	25	40	5	n.d.	503.2	3680.4	1059.8	n.d.
Station 12_Patna (B)	819.6 ± 38.0	n.a.a.	n.a.a.	n.a.a.	884.0 ± 38.0	15	200	15	n.d.	913.9	3832.5	701.4	n.d.
Station 13_Patna (B)	216.8 ± 19.3	n.a.a.	n.a.a.	n.a.a.	581.0 ± 19.3	17	100	10	n.d.	181.5	535.7	229.7	n.d.
Station 14_Patna (B)	n.d.	n.a.a.	n.a.a.	n.a.a.	297.8 ± 19.8	16	100	15	n.d.	n.d.	n.d.	n.d.	n.d.
Station 15_Patna (B)	82.2 ± 4.5	n.a.a.	n.a.a.	n.a.a.	71.8 ± 4.5	23	10	5	n.d.	120.1	2624.2	862.1	n.d.

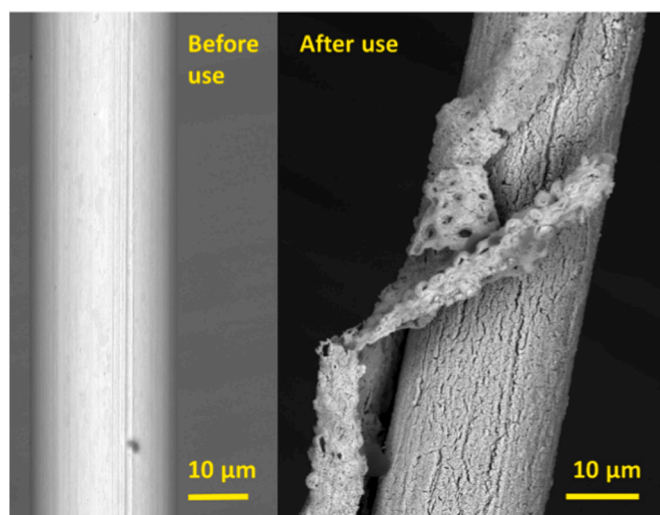


Fig. 7. BSE micrographs of the Au WireBond sensor showing the smooth surface of a new electrode and the damaged surface of the electrode used in India 2022. (25 μm diameter).

4. Conclusions

This study has shown that total As, i.e. As(III) and As(V), can be detected over a wide pH range (including neutral pH) using anodic stripping voltammetry, in the presence of KMnO_4 , with a portable device using a sturdy electrode, sensitive and a convivial method that can be used with non-experts. After investigating a range of buffers, the optimal electrolyte was found to be a chloride containing acetate buffer (CLAC). Detection limits were sub-ppb level with deposition time in seconds only, and the linear range was sufficient for quantification of all field samples using the method of standard. No purging was needed, thereby decreasing the analysis time and improving the portability of the sensor. Measurements in the CLAC buffer were generally favourable over analysis in 0.1 M HCl, considering that the interfering effect of copper is reduced significantly, a better agreement with benchmark ICP-MS was observed and in general, it was more sensitive as compared to analysis in 0.1 M HCl. Addition of 1 mM EDTA did not interfere significantly with analysis, indicating that the chelating agent can be used as an additive at the time of sampling to prevent Fe (and/or Mn) precipitation in reducing groundwaters such as in India. The method was successfully applied to both reducing groundwaters in India (i.e. As(III) rich) and oxidising groundwaters in Mexico (i.e. As(V) rich), providing good correlation with ICP-MS measurements. The gold microwire electrodes are sturdy, easy to manipulate and can be used for a long time; a single electrode here was used for the analysis of more than 220 Mexican groundwater samples by ASV, each sample being measured by standard addition with triplicate measurements (9 measurements per sample giving more than 2000 ASV scans for a single electrode). The standard addition procedure takes about 10 min when using a short deposition time of 10 or 30 s. It was found that the electrode sensitivity is somewhat affected by the deposition time, but the major controls on sensitivity are electrode usage and groundwater chemistry. Thus, the results of this work demonstrate that this new method is a promising technique that can easily and quickly measure arsenic concentration in groundwater.

CRedit authorship contribution statement

Martijn Eikelboom: Conceptualization, Methodology, Formal analysis, Investigation, Writing – original draft, Visualization. **Yaxuan Wang:** Investigation. **Gemma Portlock:** Methodology, Investigation. **Arthur Gourain:** Conceptualization, Methodology, Investigation. **Joseph Gardner:** Investigation, Resources, Writing – review & editing.

Jay Bullen: Conceptualization, Methodology, Writing – review & editing, Supervision. **Paul Lewtas:** Conceptualization, Methodology, Software, Resources. **Matthieu Carriere:** Resources, Writing – review & editing. **Alexandra Alvarez:** Resources, Writing – review & editing. **Arun Kumar:** Investigation, Resources. **Shane O’Prey:** Resources. **Tamás Tölgyes:** Resources. **Dario Omanović:** Methodology, Resources, Validation. **Subhamoy Bhowmick:** Investigation, Resources, Supervision, Writing – review & editing. **Dominik Weiss:** Supervision, Writing – review & editing. **Pascal Salaun:** Conceptualization, Methodology, Validation, Formal analysis, Investigation, Resources, Writing – original draft, Writing – review & editing, Supervision, Project administration, Funding acquisition.

Declaration of competing interest

The authors declare that they have no known competing financial interests or personal relationships that could have appeared to influence the work reported in this paper.

Data availability

Data will be made available on request.

5. Acknowledgements

Martijn Eikelboom was supported by the University of Liverpool.

Appendix A. Supplementary data

Supplementary data to this article can be found online at <https://doi.org/10.1016/j.aca.2023.341589>.

References

- [1] A. Kumar, et al., Assessment of disease burden in the arsenic exposed population of Chapar village of Samastipur district, Bihar, India, and related mitigation initiative, *Environ. Sci. Pollut. Res. Int.* 29 (18) (2022) 27443–27459.
- [2] M.T. Alarcon-Herrera, et al., Co-occurrence, possible origin, and health-risk assessment of arsenic and fluoride in drinking water sources in Mexico: geographical data visualization, *Sci. Total Environ.* 698 (2020), 134168.
- [3] K. Rangel-Moreno, et al., Prevalence of type 2 diabetes mellitus in relation to arsenic exposure and metabolism in Mexican women, *Environ. Res.* 210 (2022), 112948.
- [4] M. Chakraborty, A. Mukherjee, K.M. Ahmed, A review of groundwater arsenic in the bengal basin, Bangladesh and India: from source to sink, *Current Pollution Reports* 1 (4) (2015) 220–247.
- [5] WHO, *Guidelines for Drinking-Water Quality*, fourth ed., 2022 with 1st and 2nd addendum.
- [6] J.S. Uppal, Q. Zheng, X.C. Le, Arsenic in drinking water—recent examples and updates from Southeast Asia, *Current Opinion in Environmental Science & Health* 7 (2019) 126–135.
- [7] J. Ortiz Letechipia, et al., Aqueous arsenic speciation with hydrogeochemical modeling and correlation with fluorine in groundwater in a semiarid region of Mexico, *Water* 14 (4) (2022).
- [8] A.K. Kundu, et al., Optimisation of laboratory arsenic analysis for groundwaters of West Bengal, India and possible water testing strategy, *Int. J. Environ. Anal. Chem.* 98 (5) (2018) 440–452.
- [9] A. Ahmad, P. Bhattacharya, Arsenic in drinking water: is 10 µg/L a safe limit? *Current Pollution Reports* 5 (1) (2019) 1–3.
- [10] A. Ahmad, et al., Arsenite removal in groundwater treatment plants by sequential Permanganate–Ferric treatment, *J. Water Proc. Eng.* 26 (2018) 221–229.
- [11] B. Biswas, et al., Arsenic exposure from drinking water and staple food (rice): a field scale study in rural Bengal for assessment of human health risk, *Ecotoxicol. Environ. Saf.* 228 (2021), 113012.
- [12] S. Bhowmick, et al., Arsenic mobilization in the aquifers of three physiographic settings of West Bengal, India: understanding geogenic and anthropogenic influences, *J. Hazard Mater.* 262 (2013) 915–923.
- [13] A. Biswas, et al., Groundwater chemistry and redox processes: depth dependent arsenic release mechanism, *Appl. Geochem.* 26 (4) (2011) 516–525.
- [14] C.C. Osuna-Martínez, et al., Arsenic in waters, soils, sediments, and biota from Mexico: an environmental review, *Sci. Total Environ.* (2021) 752.
- [15] P.S.K. Knappett, et al., Rising arsenic concentrations from dewatering a geothermally influenced aquifer in central Mexico, *Water Res.* 185 (2020), 116257.
- [16] K. Gibbon-Walsh, et al., Voltammetric determination of arsenic in high iron and manganese groundwaters, *Talanta* 85 (3) (2011) 1404–1411.
- [17] L.C. Roberts, et al., Spatial distribution and temporal variability of arsenic in irrigated rice fields in Bangladesh. 1. Irrigation water, *Environ. Sci. Technol.* 41 (17) (2007) 5960–5966.
- [18] D.Q. Hung, O. Nekrassova, R.G. Compton, Analytical methods for inorganic arsenic in water: a review, *Talanta* 64 (2) (2004) 269–277.
- [19] H. Jiang, et al., Hollow fiber liquid phase microextraction combined with electrothermal atomic absorption spectrometry for the speciation of arsenic (III) and arsenic (V) in fresh waters and human hair extracts, *Anal. Chim. Acta* 634 (1) (2009) 15–21.
- [20] L. Rajakovic, et al., Analytical methods for arsenic speciation analysis, *J. Serb. Chem. Soc.* 78 (10) (2013) 1461–1479.
- [21] M. Guo, et al., HPLC-HG-AFS determination of arsenic species in acute promyelocytic leukemia (APL) plasma and blood cells, *J. Pharm. Biomed. Anal.* 145 (2017) 356–363.
- [22] J. Ma, et al., Speciation and detection of arsenic in aqueous samples: a review of recent progress in non-atomic spectrometric methods, *Anal. Chim. Acta* 831 (2014) 1–23.
- [23] G.M. Alves, et al., Simultaneous electrochemical determination of arsenic, copper, lead and mercury in unpolluted fresh waters using a vibrating gold microwire electrode, *Anal. Chim. Acta* 703 (1) (2011) 1–7.
- [24] J.C. Bullen, et al., Low-cost electrochemical detection of arsenic in the groundwater of Guanajuato state, central Mexico using an open-source potentiostat, *PLoS One* 17 (1) (2022), e0262124.
- [25] K. Gibbon-Walsh, P. Salaun, C.M. van den Berg, Determination of arsenate in natural pH seawater using a manganese-coated gold microwire electrode, *Anal. Chim. Acta* 710 (2012) 50–57.
- [26] P. Salaun, K. Gibbon-Walsh, C.M. van den Berg, Beyond the hydrogen wave: new frontier in the detection of trace elements by stripping voltammetry, *Anal. Chem.* 83 (10) (2011) 3848–3856.
- [27] P. Salaun, et al., Determination of arsenic and antimony in seawater by voltammetric and chronopotentiometric stripping using a vibrated gold microwire electrode, *Anal. Chim. Acta* 746 (2012) 53–62.
- [28] P. Salaun, B. Planer-Friedrich, C.M. van den Berg, Inorganic arsenic speciation in water and seawater by anodic stripping voltammetry with a gold microelectrode, *Anal. Chim. Acta* 585 (2) (2007) 312–322.
- [29] G. Forsberg, J.W. O’Laughlin, R.G. Megargle, Determination of arsenic by anodic stripping voltammetry and differential pulse anodic stripping voltammetry, *Anal. Chem.* 47 (9) (1975).
- [30] E.A. Zakharova, et al., Methods of the determination of inorganic arsenic species by stripping voltammetry in weakly alkaline media, *J. Anal. Chem.* 71 (8) (2016) 823–833.
- [31] S. Antonova, E. Zakharova, Inorganic arsenic speciation by electroanalysis. From laboratory to field conditions: a mini-review, *Electrochem. Commun.* 70 (2016) 33–38.
- [32] E.A. Zakharova, et al., Investigations into the speciation of inorganic arsenic in weakly alkaline medium by voltammetry, *Electroanalysis* 27 (4) (2015) 890–901.
- [33] E.A. Zakharova, et al., Speciation of arsenic(III) and arsenic(V) by manganese-mediated stripping voltammetry at gold microelectrode ensemble in neutral and basic medium, *Int. J. Environ. Anal. Chem.* 94 (14–15) (2014) 1478–1498.
- [34] E. Zakharova, et al., Gold microelectrode ensembles: cheap, reusable and stable electrodes for the determination of arsenic (V) under aerobic conditions, *Int. J. Environ. Anal. Chem.* 93 (11) (2013) 1105–1115.
- [35] G.N. Noskova, et al., Electrodeposition and stripping voltammetry of arsenic(III) and arsenic(V) on a carbon black–polyethylene composite electrode in the presence of iron ions, *J. Solid State Electrochem.* 16 (7) (2012) 2459–2472.
- [36] R. Feeney, S.P. Kounaves, On-site analysis of arsenic in groundwater using a microfabricated gold ultramicroelectrode array, *Anal. Chem.* 72 (10) (2000) 2222–2228.
- [37] S.P. Méndez Cortés, et al., Square wave anodic stripping voltammetry determination of arsenic (III) onto carbon electrodes by means of Co-deposition with silver, *Journal of the Mexican Chemical Society* 62 (2) (2018).
- [38] Y. Nagaoka, et al., Selective detection of as(V) with high sensitivity by as-deposited boron-doped diamond electrodes, *Chem. Lett.* 39 (10) (2010) 1055–1057.
- [39] A.O. Simm, C.E. Banks, R.G. Compton, The electrochemical detection of arsenic(III) at a silver electrode, *Electroanalysis* 17 (19) (2005) 1727–1733.
- [40] M. Yang, et al., Electrochemical determination of arsenic(III) with ultra-high anti-interference performance using Au–Cu bimetallic nanoparticles, *Sensor. Actuator. B Chem.* 231 (2016) 70–78.
- [41] S. Sanlloriente-Mendez, O. Dominguez-Renedo, M.J. Arcos-Martínez, Immobilization of acetylcholinesterase on screen-printed electrodes. Application to the determination of arsenic(III), *Sensors* 10 (3) (2010) 2119–2128.
- [42] P.S.P. Singh, Role of PtO on the oxidation of Arsenic (III) at Pt RDE in 1M H₂SO₄ and 1M Na₂SO₄ through linear sweep voltammetry technique, *Int. J. Electrochem. Sci.* 2 (2007) 311–320.
- [43] K. Torres-Rivero, et al., Direct as(V) determination using screen-printed electrodes modified with silver nanoparticles, *Nanomaterials* 10 (7) (2020).
- [44] J.C. Bullen, et al., Portable and rapid arsenic speciation in synthetic and natural waters by an As(V)-selective chemisorbent, validated against anodic stripping voltammetry, *Water Res.* 175 (2020), 115650.
- [45] P.N.D. Duoc, et al., A novel electrochemical sensor based on double-walled carbon nanotubes and graphene hybrid thin film for arsenic(V) detection, *J. Hazard Mater.* 400 (2020), 123185.
- [46] K. Gibbon-Walsh, P. Salaun, C.M. van den Berg, Arsenic speciation in natural waters by cathodic stripping voltammetry, *Anal. Chim. Acta* 662 (1) (2010) 1–8.
- [47] L. Meites, Polarographic characteristics of +3 and +5 arsenic in hydrochloric acid solutions, *J. Am. Chem. Soc.* (1954).

- [48] S.B. Rasul, et al., Electrochemical measurement and speciation of inorganic arsenic in groundwater of Bangladesh, *Talanta* 58 (1) (2002) 33–43.
- [49] Y.C. Sun, J. Mierzwa, M.H. Yang, New method of gold-film electrode preparation for anodic stripping voltammetric determination of arsenic (III and V) in seawater, *Talanta* 44 (8) (1997) 1379–1387.
- [50] Y. He, Y. Zheng, D.C. Locke, Cathodic stripping voltammetric analysis of arsenic species in environmental water samples, *Microchem. J.* 85 (2) (2007) 265–269.
- [51] A. Penezić, et al., Spatial variability of arsenic speciation in the Gironde Estuary: emphasis on dynamic (potentially bioavailable) inorganic arsenite and arsenate fractions, *Mar. Chem.* (2020) 223.
- [52] P. Salaun, C.M. van den Berg, Voltammetric detection of mercury and copper in seawater using a gold microwire electrode, *Anal. Chem.* 78 (14) (2006) 5052–5060.
- [53] A. Cheng, et al., Investigating arsenic contents in surface and drinking water by voltammetry and the method of standard additions, *J. Chem. Educ.* 93 (11) (2016) 1945–1950.
- [54] B. Pernet-Coudrier, et al., Simple and simultaneous determination of glutathione, thioacetamide and refractory organic matter in natural waters by DP-CSV, *Sci. Total Environ.* 463–464 (2013) 997–1005.
- [55] A.J. Bard, *Standard Potentials in Aqueous Solution*, Vol. first ed., Routledge, New York, 1985.
- [56] Sharma, G.M.S.C.V.K, *Tables of Standard Electrode Potentials*, 1978.
- [57] Z.-G. Liu, X.-J. Huang, Voltammetric determination of inorganic arsenic, *TrAC, Trends Anal. Chem.* 60 (2014) 25–35.
- [58] Z.G. Liu, et al., Role of Fe(III) in preventing humic interference during As(III) detection on gold electrode: spectroscopic and voltammetric evidence, *J. Hazard Mater.* 267 (2014) 153–160.
- [59] J. Buschmann, et al., Arsenite and arsenate binding to dissolved humic acids: influence of pH, type of humic acid, and aluminum, *Environ. Sci. Technol.* 40 (19) (2006) 6015–6020.
- [60] S. Dixit, J.G. Hering, Comparison of arsenic(V) and arsenic(III) sorption onto iron oxide minerals: implications for arsenic mobility, *Environ. Sci. Technol.* 37 (18) (2003) 4182–4189.
- [61] A. Ahmad, et al., Impact of phosphate, silicate and natural organic matter on the size of Fe(III) precipitates and arsenate co-precipitation efficiency in calcium containing water, *Separ. Purif. Technol.* (2020) 235.